Clustering, lensing and ISW-RS from the neutrino DEMNUni simulations

Carmelita Carbone

INAF - Astronomical Observatory of Brera

This project has received funding from the European Union's Seventh Framework Programme for research, technological development and demonstration under grant agreement no 291521

28th Texas Symposium on Relativistic Astrophysics, 13-18 December 2015, Geneva

Outline

- DEMNUni: the "Dark Energy and Massive Neutrino Universe" project
- "DEMNUni: The clustering of large-scale structures in the presence of massive neutrinos", Castorina et al 2015, JCAP07(2015)043
- "DEMNUni: ISW, Rees-Sciama, and weak-lensing in the presence of massive neutrinos", Carbone et al. in prep

DEMNUni simulations (PI Carbone)

- **5×10^6 cpu-hours on BGQ/FERMI at CINECA**
- **4 mixed dark matter cosmological simulations for CMB and LSS analysis in the presence of massive neutrinos**
- **Planck cosmology, M_ν=0, 0.17, 0.3, 0.53 eV (and w0-wa the next yr)**
- **Gadget-3 with ν-particle component (Viel et al. 2010)**
- **box-side size: 2 Gpc/h**
- **particle number: 2×2048^3 (CDM+ν)**
- **CDM mass: $8 \times 10^{10}\ M_\odot/h$ (neutrino particle mass depends on M_ν, 1% at k=1)**
- **softening length: 20 kpc/h**
- **starting redshift: z_{in}=99**

$$k_{\rm nr} = 0.018 (m_\nu/1{\rm eV})^{1/2} \Omega_m^{1/2} h/{\rm Mpc}$$

Castorina, CC et al. 2015

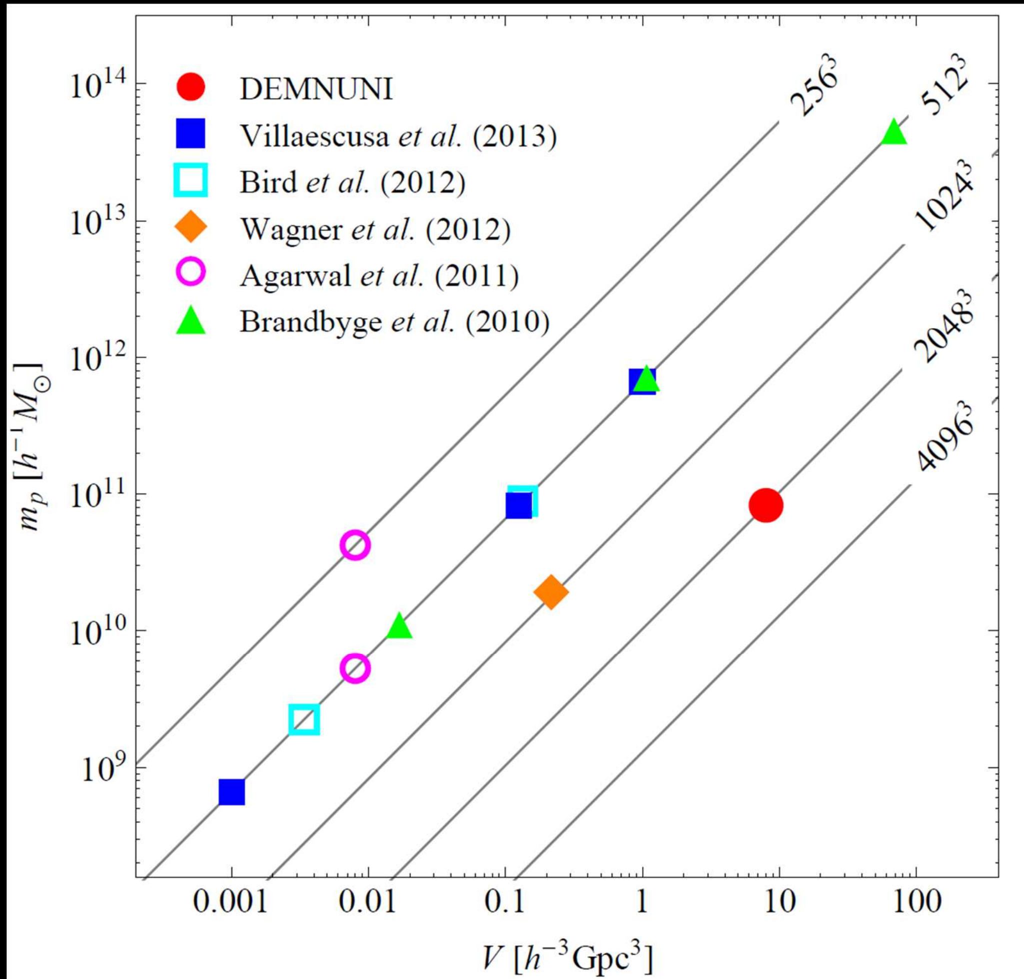

Comparison between the DEMNUni runs and previous, recent simulations of massive neutrino cosmologies in terms of cold dark matter mass resolution and volume

DEMNUni matter power spectra for M_ν=0.3 eV

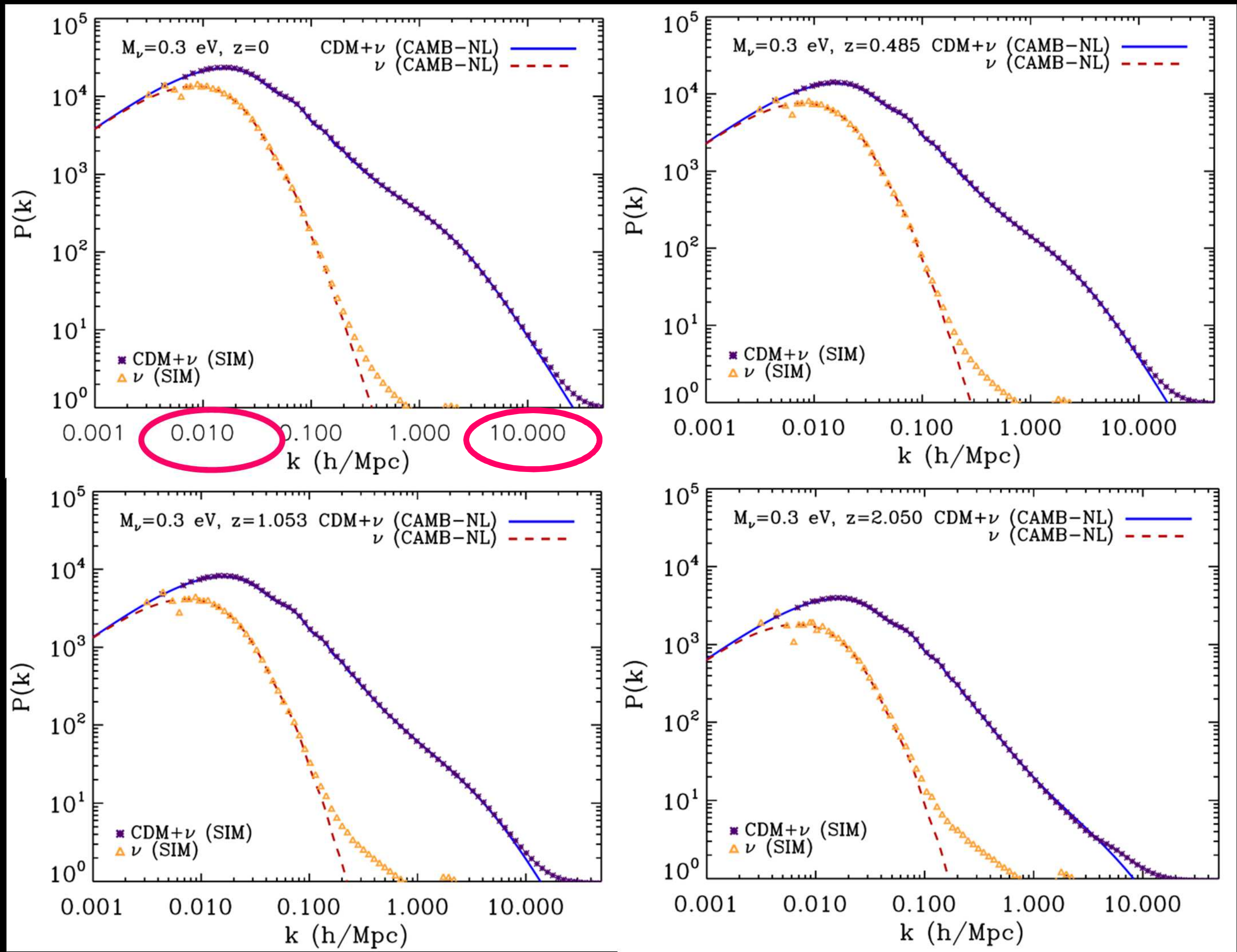

The large volume and mass resolution of the DEMNUni simulations allow to test different probes, and their combinations, in massive neutrino cosmologies, at the level of accuracy required by current and future galaxy surveys.

Total matter P(k) ratios wrt LCDM

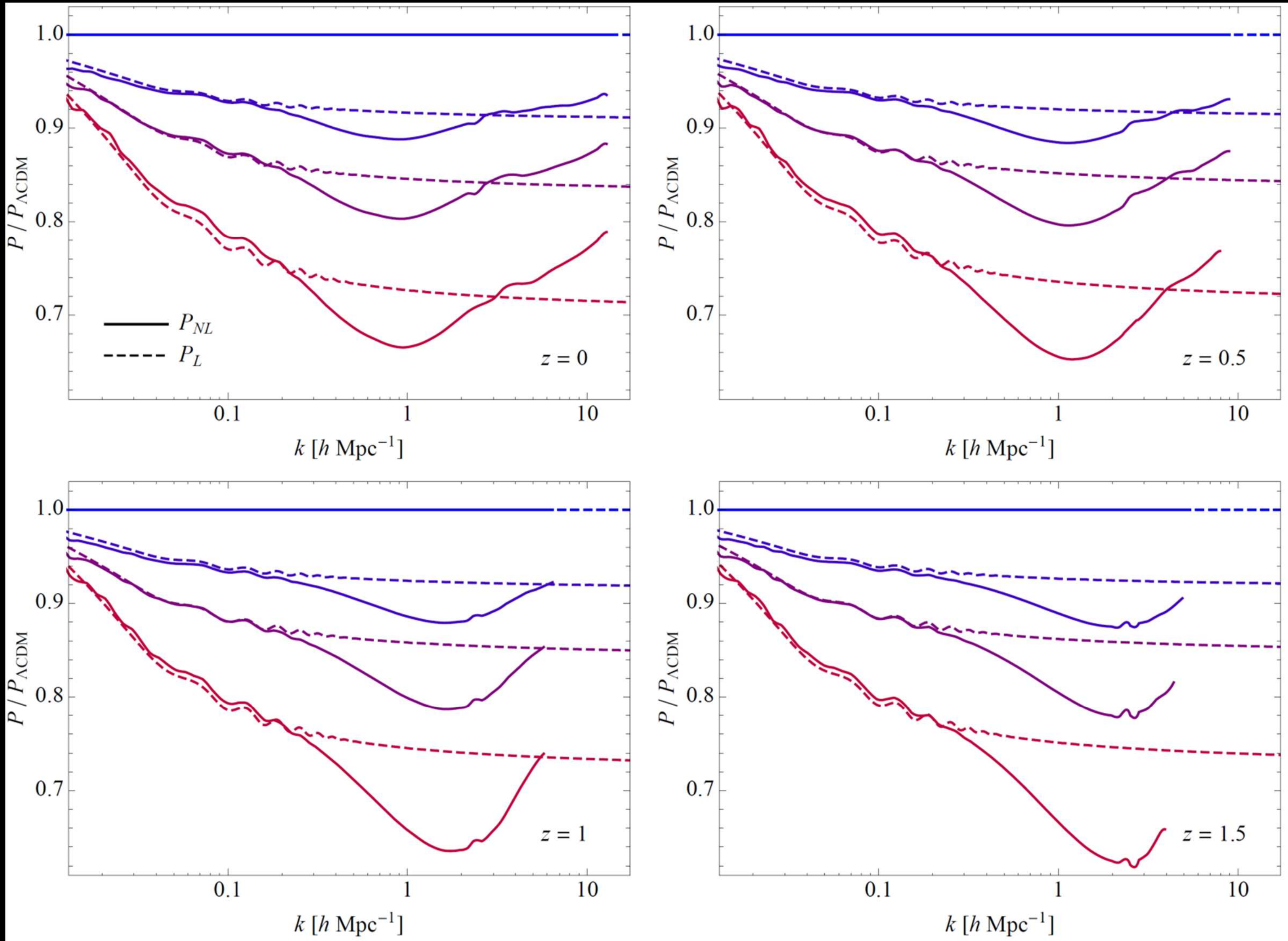

$$k_{\rm fs}(z) = 0.82 H(z)/H_0/(1+z)^2 (m_\nu/1\text{eV}) \;\; h\,\text{Mpc}^{-1}$$

Different contributions to the total matter P(k)

Castorina, CC et al. 2015

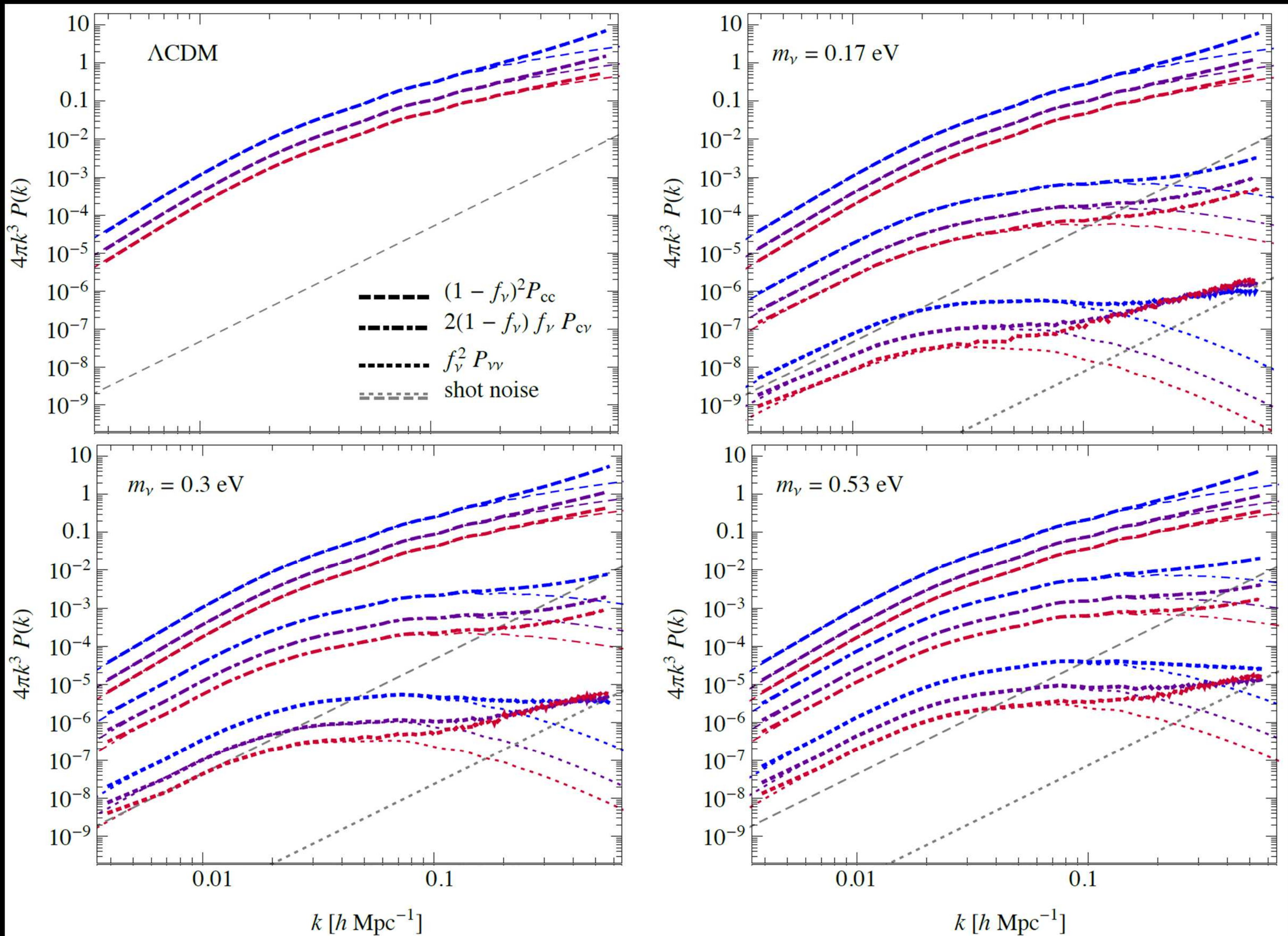

$$P_m(k;z) = (1-f_\nu)^2\, P_{cb}(k;z) + 2\,(1-f_\nu) f_\nu\, P_{cb,\nu}(k;z) + f_\nu^2\, P_\nu(k;z)$$

$P_m(k)$ is described at the 1% level accuracy up to k=1*h*/Mpc, assuming the nonlinear evolution of CDM alone, and the linear prediction for the other components

Perturbation theory vs Simulations

Castorina, CC et al. 2015

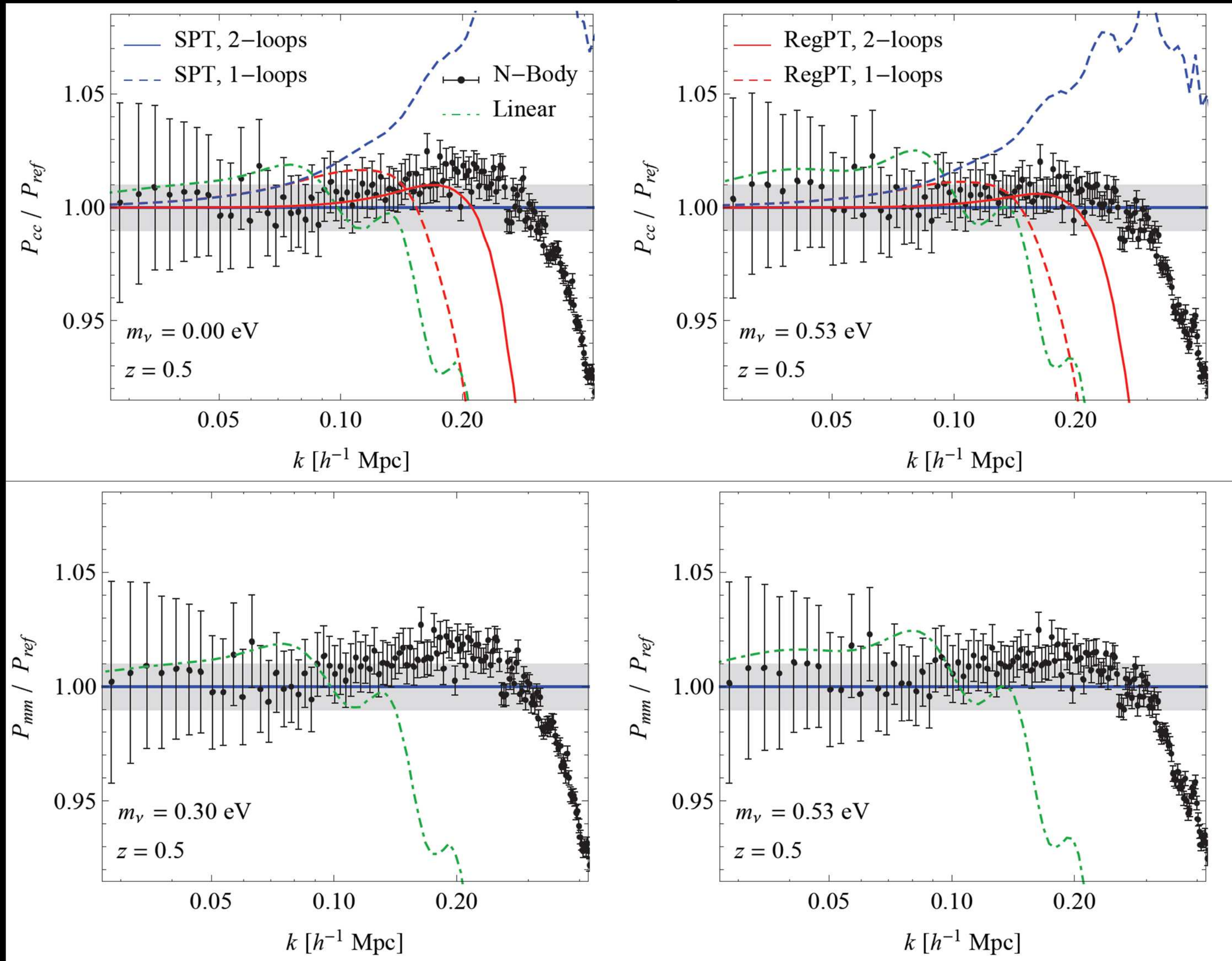

$$P^{PT}_{mm}(k) = (1-f_\nu)^2\, P^{PT}_{cc}(k) + 2\,(1-f_\nu)\, f_\nu\, P^{L}_{c\nu}(k) + f_\nu^2\, P^{L}_{\nu\nu}(k)$$

(RegularizedPT: Bernardau et al 2008, Taruya et al 2012)

Here the neutrino induced scale-dependence is limited to the linear growth factor, *D(k,z)*, while the perturbation kernels are standard ones. PT works better with M_ν

Modifications to Halofit

Castorina, CC et al. 2015

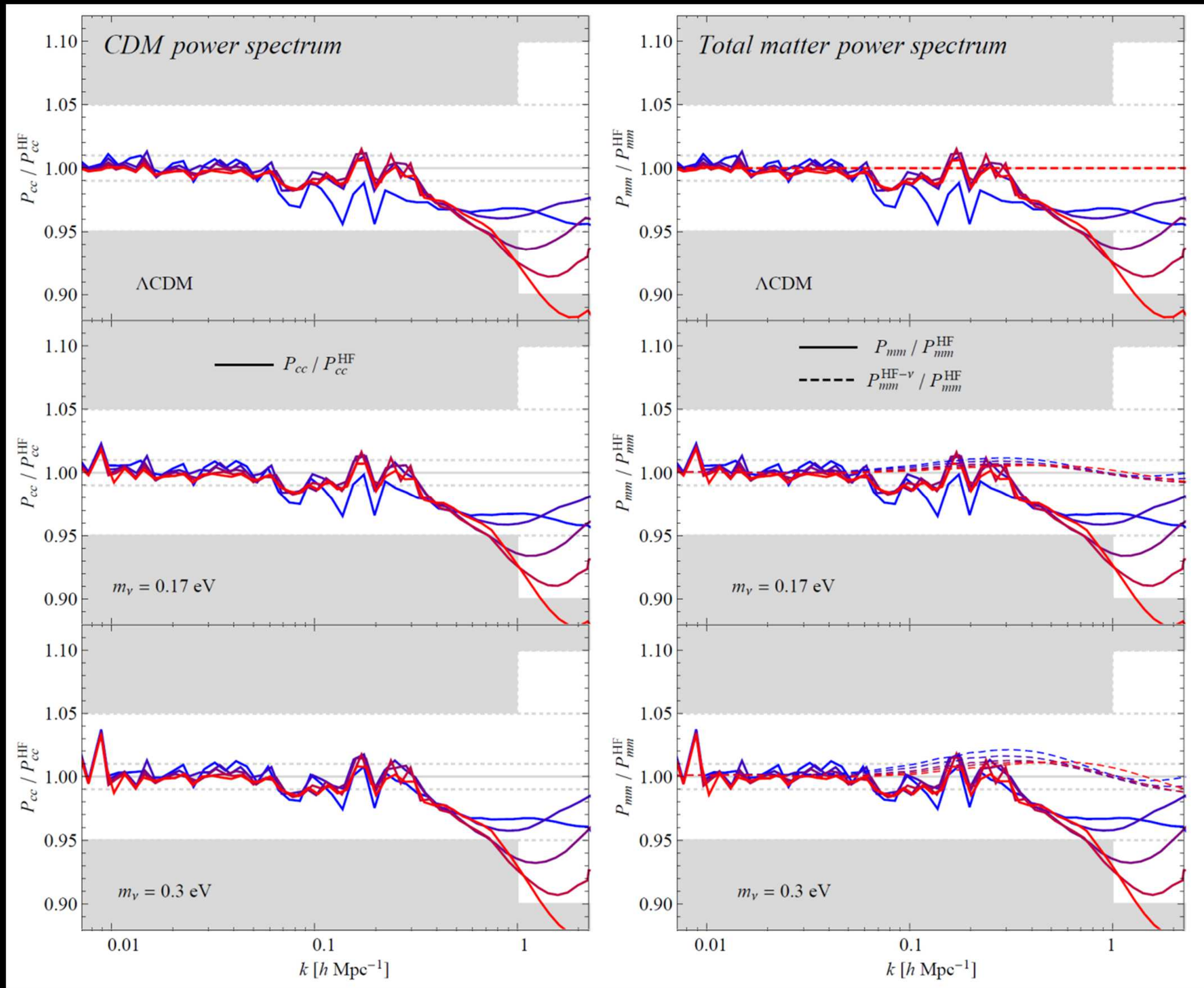

$$P^{HF}_{mm}(k) \equiv (1-f_\nu)^2\, P^{HF}_{cc}(k) + 2\, f_\nu\, (1-f_\nu)\, P^{L}_{c\nu}(k) + f_\nu^2\; P^{L}_{\nu\nu}(k)$$

$$P^{HF}_{cc}(k) \;=\; \mathcal{F}_{HF}[P^{L}_{cc}(k)]$$

HALOFIT mapping only for CDM, other contributions are assumed to be linear.
Shaded areas denote regions beyond the accurracy expected from Halofit.

Halo Mass Function: FoF

Castorina, CC et al. 2015

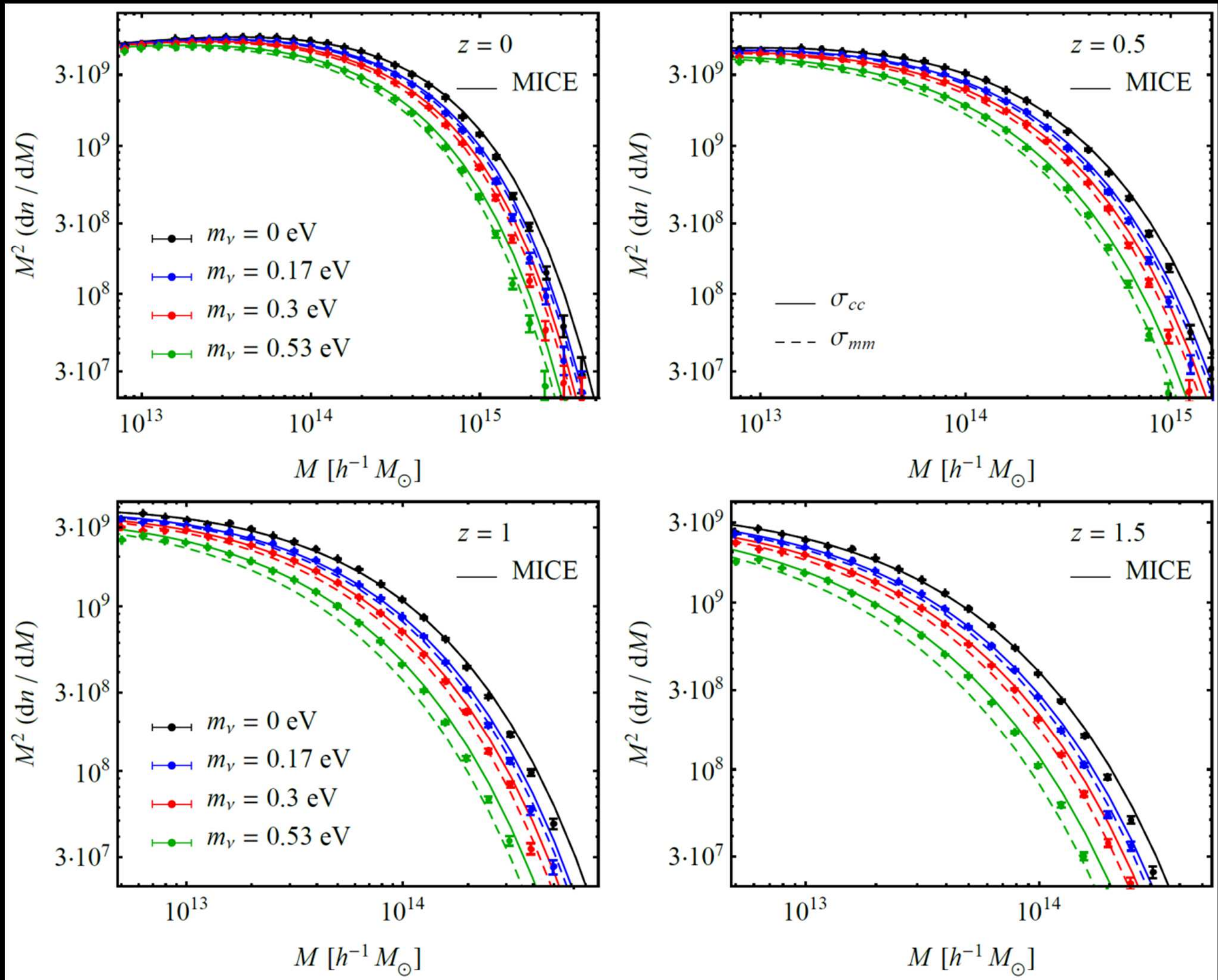

We recover the ρ_{cc} and σ_{cc} prescription from Ichiki&Takada (2012) and Castorina et al (2014) for the MICE formula. Note the large halo-mass range.

Halo Mass Function: FoF (MICE) vs SO (Tinker)

Castorina, CC et al. 2015

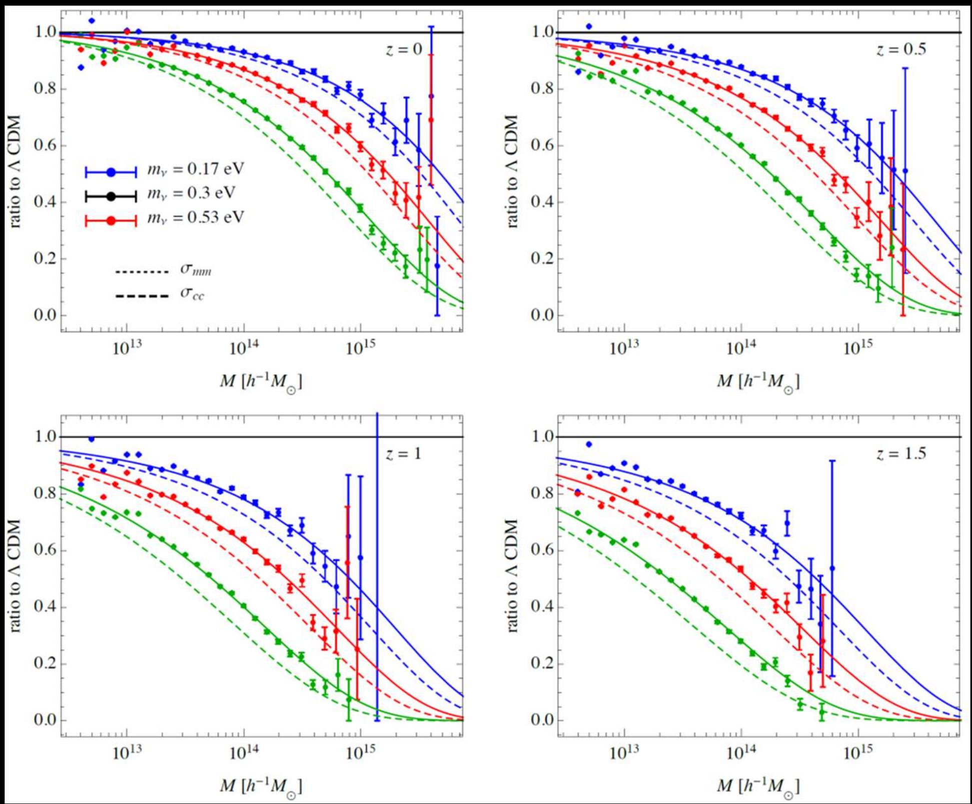

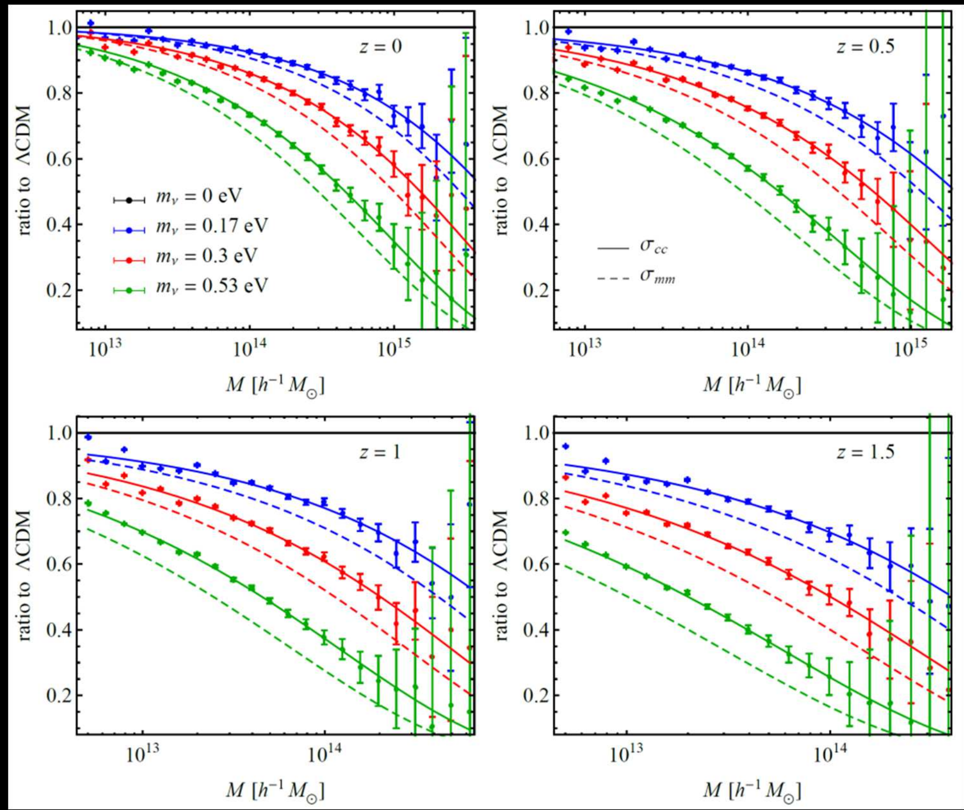

The ρ_{cc} and σ_{cc} prescriptions allow to recover the theoretical MF for both FoF and SO halos

Same conclusions for the bias

Castorina, CC et al. 2015

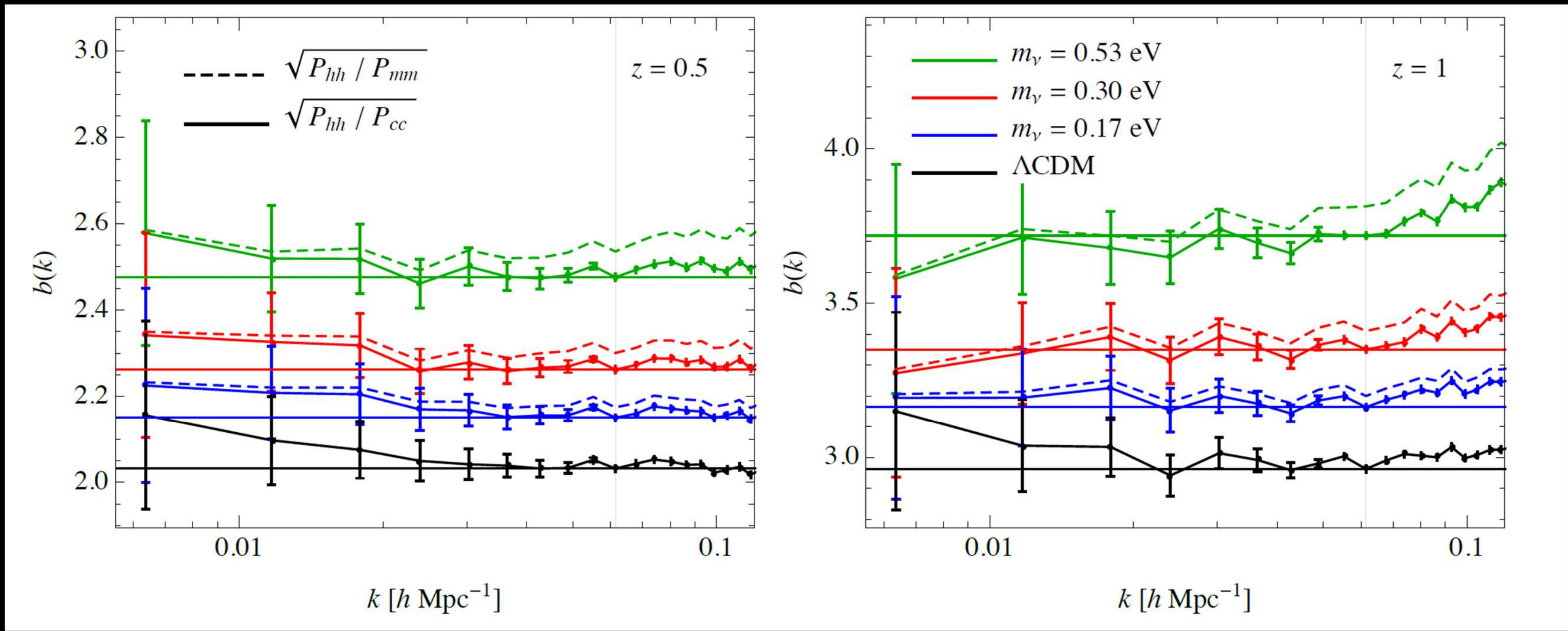

$$b_c = \sqrt{\frac{P_{hh}}{P_{cc}}}$$

$$b_m = \sqrt{\frac{P_{hh}}{P_{mm}}}$$

The σ_{cc} prescription mitigates the ν-induced scale dipendence of the bias at intermediate scales. The halo bias defined with respect to DM presents a spurious scale-dependence due to the difference between the cold and total matter power spectra.

Measurements in redshift space

Castorina, CC et al. 2015

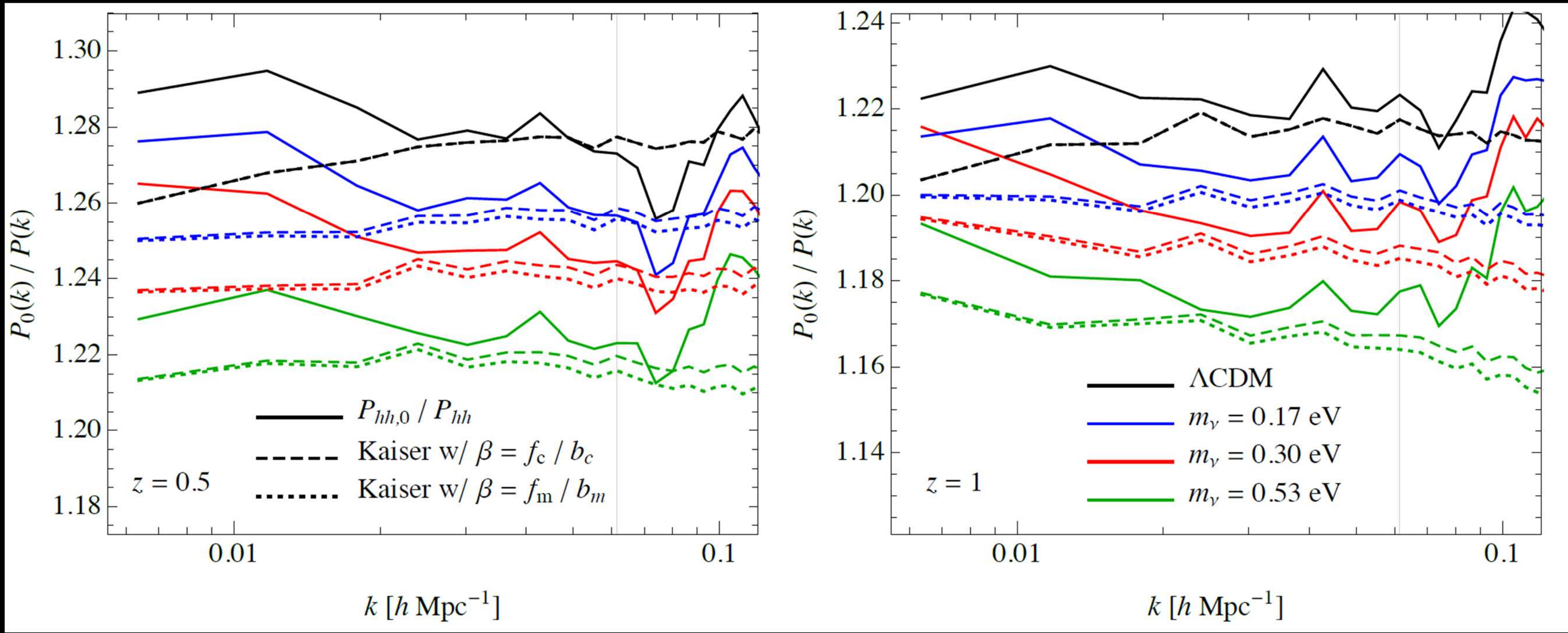

$$P_{hh,s}(\vec{k}) = (1 + \beta\mu^2)^2\, P_{hh}(k) = \sum_{l=0,2,4} P_{hh,\ell}\, L_\ell(\mu)$$

$$P_{hh,0}(k) = \left(1 + \frac{2}{3}\beta + \frac{1}{5}\beta^2\right) P_{hh}(k)$$

$$P_{hh,2}(k) = \left(\frac{4}{3}\beta + \frac{4}{7}\beta^2\right) P_{hh}(k)$$

$$P_{hh,4}(k) = \frac{8}{35}\beta^2 P_{hh}(k),$$

f_c and σ_{cc} prescriptions work slightly better than f_m and σ_{mm} (velocity bias effects are neglected)

The scale dependent growth-rate

Using b_{m} instead of b_{cc} implies a systematic error on the determination of the growth rate at the level of 1-2%

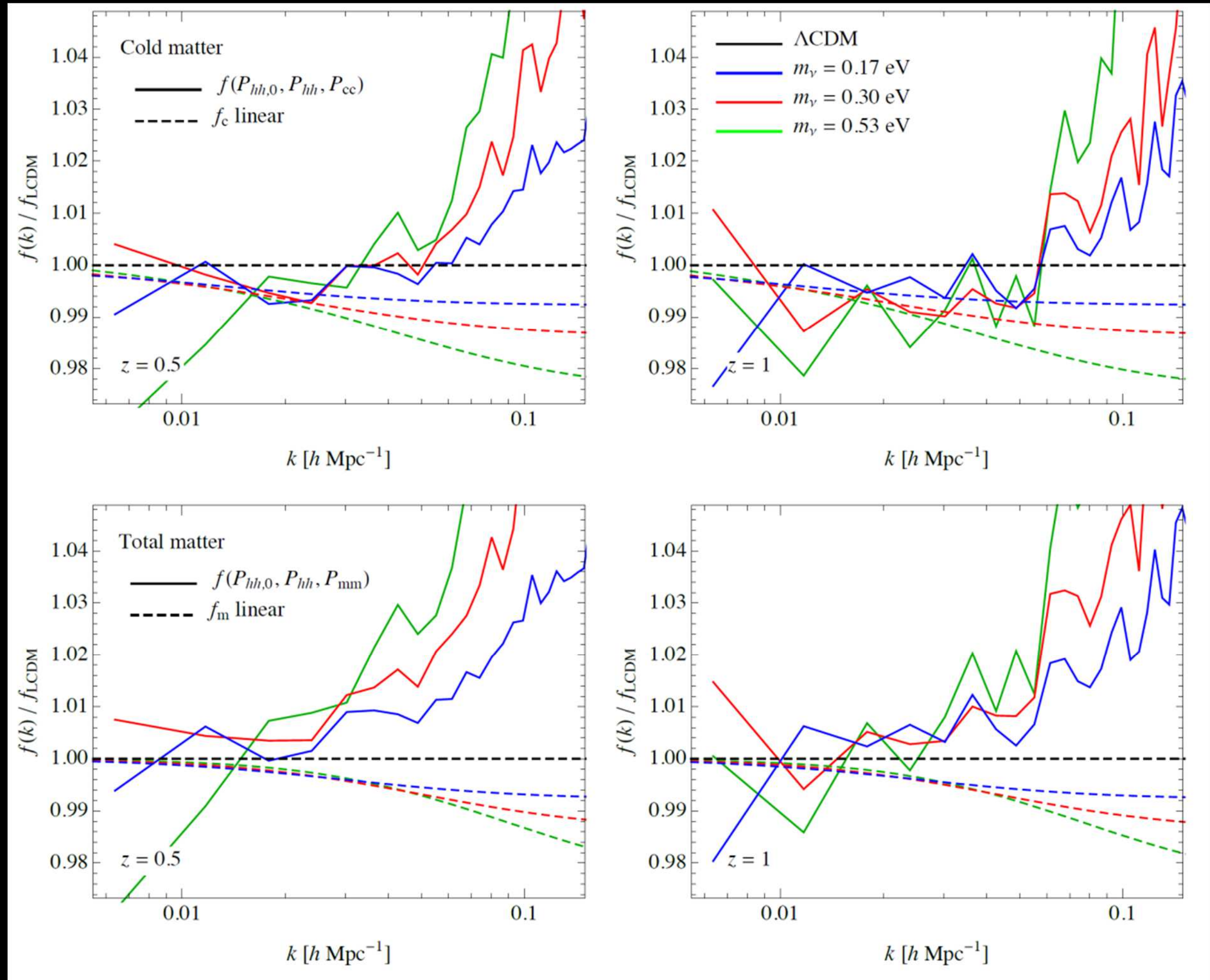

$$\beta \equiv f/b$$

$$f(a) \equiv \frac{d \ln D(a)}{d \ln a}$$

$$f(k) = \sqrt{\frac{P_{hh}(k)}{P_{\underset{(mm)}{cc}}(k)}}\,\frac{1}{3}\left[\sqrt{45\,\frac{P_{hh,0}(k)}{P_{hh}(k)} - 20} - 5\right]$$

Castorina, CC et al. 2015

Lensing and ISW-RS quantities

$$\Psi(\hat{\mathbf{n}}) \equiv -2 \int_0^{r_*} \frac{r_* - r}{r_* r} \frac{\Phi(r\hat{\mathbf{n}}; \eta_0 - r)}{c^2} \, \mathrm{d}r$$

Lensing potential in the small-angle scattering limit (Born approximation)

r= comoving distance
from the observer

$$\Delta T(\hat{n}) = \frac{2}{c^3} \bar{T}_0 \int_0^{r_\mathrm{L}} \dot{\Phi}(r, \hat{n}) \, a \, dr,$$

Total ISW-RS effect

$$\widetilde{X}(\hat{\mathbf{n}}) = X(\hat{\mathbf{n}} + \nabla\psi(\hat{\mathbf{n}}))$$

$$X = T, Q, U$$

Gradients in the grav. potential generated by LSS cause deviations in the CMB photon propagation from LS to us:

points in a direction **n**` actually come from points on the last scattering surface in a displaced direction **n**`= **n** $+\nabla\psi$

Planck constraints on neutrinos (95% CL)

Parameter	TT	TT+lensing	TT+lensing+ext	TT, TE, EE	TT, TE, EE+lensing	TT, TE, EE+lensing+ext
Ω_K	$-0.052^{+0.049}_{-0.055}$	$-0.005^{+0.016}_{-0.017}$	$-0.0001^{+0.0054}_{-0.0052}$	$-0.040^{+0.038}_{-0.041}$	$-0.004^{+0.015}_{-0.015}$	$0.0008^{+0.0040}_{-0.0039}$
Σm_ν [eV]	< 0.715	< 0.675	< 0.234	< 0.492	< 0.589	< 0.194
$N_{\rm eff}$	$3.13^{+0.64}_{-0.63}$	$3.13^{+0.62}_{-0.61}$	$3.15^{+0.41}_{-0.40}$	$2.99^{+0.41}_{-0.39}$	$2.94^{+0.38}_{-0.38}$	$3.04^{+0.33}_{-0.33}$
$Y_{\rm P}$	$0.252^{+0.041}_{-0.042}$	$0.251^{+0.040}_{-0.039}$	$0.251^{+0.035}_{-0.036}$	$0.250^{+0.026}_{-0.027}$	$0.247^{+0.026}_{-0.027}$	$0.249^{+0.025}_{-0.026}$
$dn_s/d\ln k$	$-0.008^{+0.016}_{-0.016}$	$-0.003^{+0.015}_{-0.015}$	$-0.003^{+0.015}_{-0.014}$	$-0.006^{+0.014}_{-0.014}$	$-0.002^{+0.013}_{-0.013}$	$-0.002^{+0.013}_{-0.013}$
$r_{0.002}$	< 0.103	< 0.114	< 0.114	< 0.0987	< 0.112	< 0.113
w	$-1.54^{+0.62}_{-0.50}$	$-1.41^{+0.64}_{-0.56}$	$-1.006^{+0.085}_{-0.091}$	$-1.55^{+0.58}_{-0.48}$	$-1.42^{+0.62}_{-0.56}$	$-1.019^{+0.075}_{-0.080}$

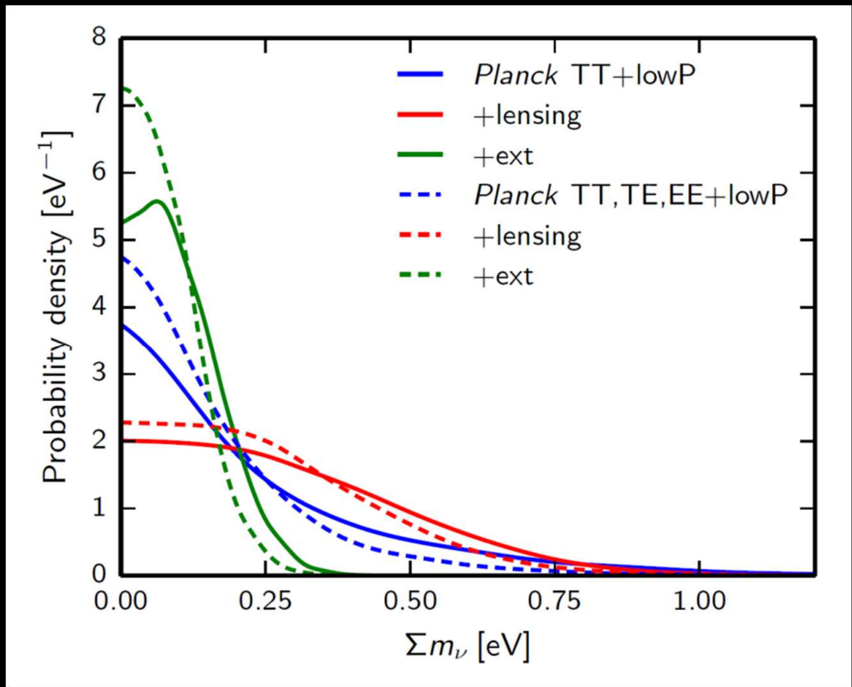

Planck-XIII (2015): the lensing reconstruction data, which directly probes the lensing power, prefers lensing amplitudes slightly below (but consistent with) the base LCDM prediction. The Planck+lensing constraint therefore pulls the constraints slightly away from zero towards higher neutrino masses. Extending the analysis up to L<900 , Planck lensing gives non-zero best-fit value for the neutrino mass:

$\sum m_\nu = 0.16^{+0.08}_{-0.11}$ eV (*Planck* TT+lowP+aggressive lensing + BAO; 68%)

Deflection angle maps for z_s=1

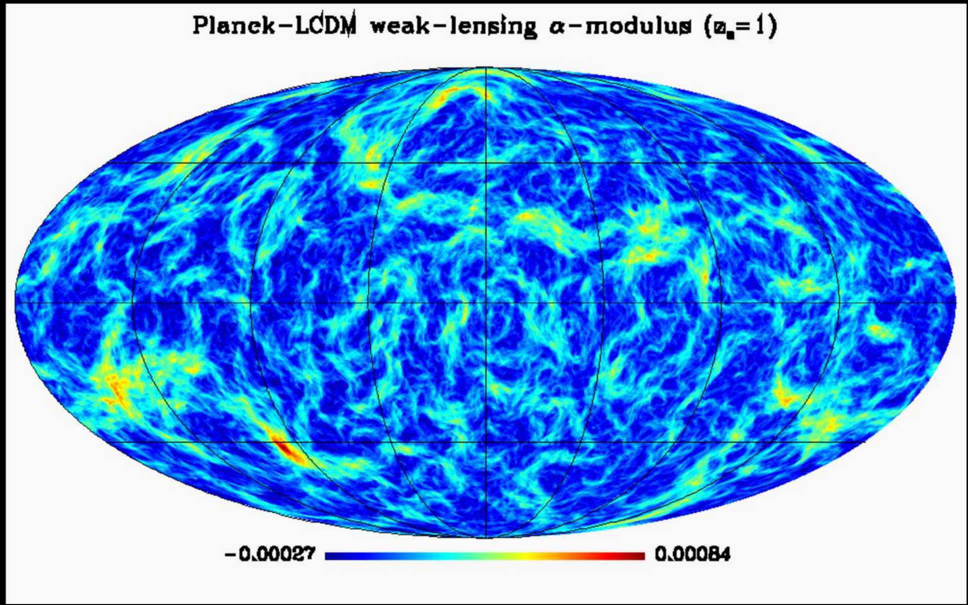

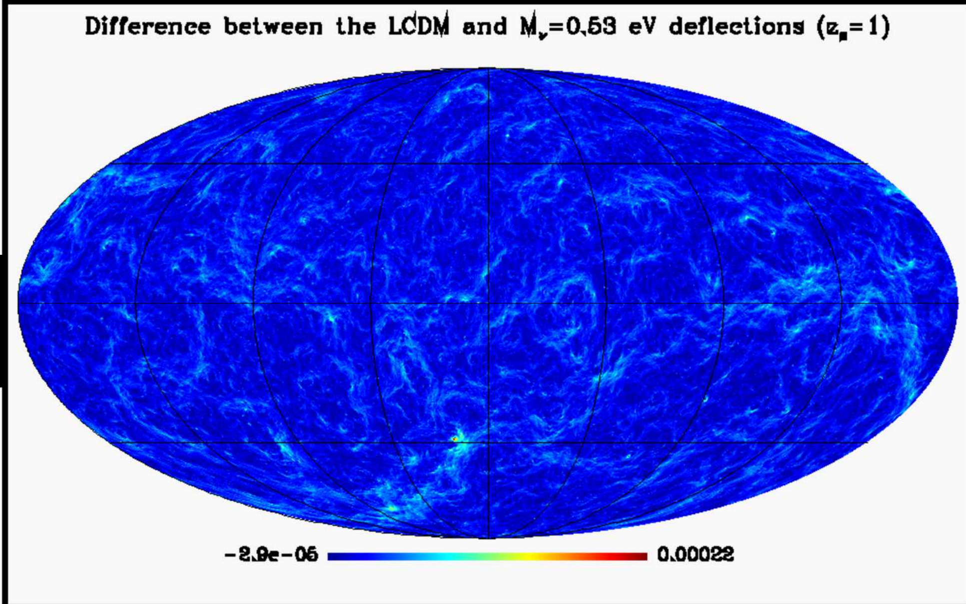

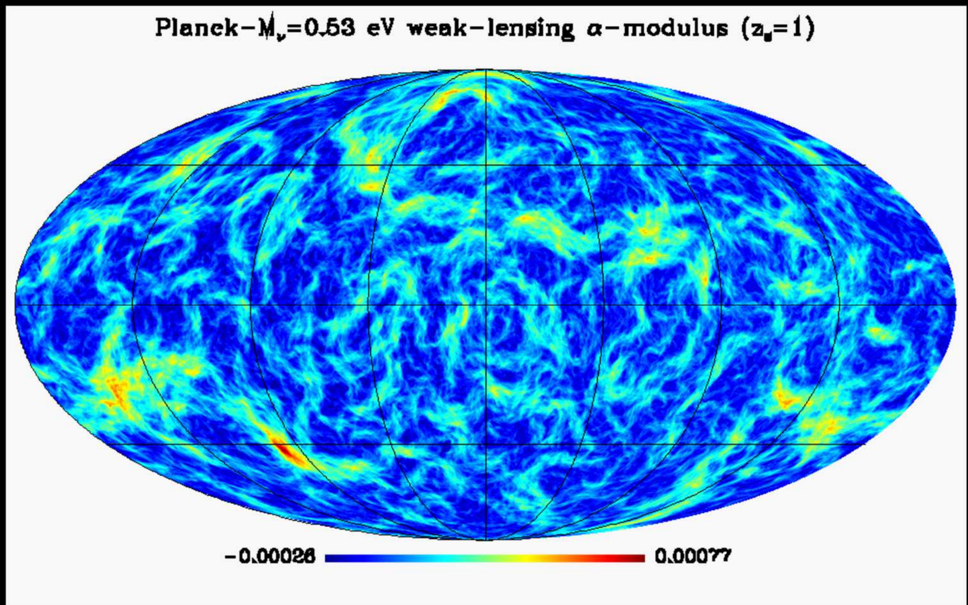

CC et al. in prep

Weak-lensing angular power spectra at different redshifts

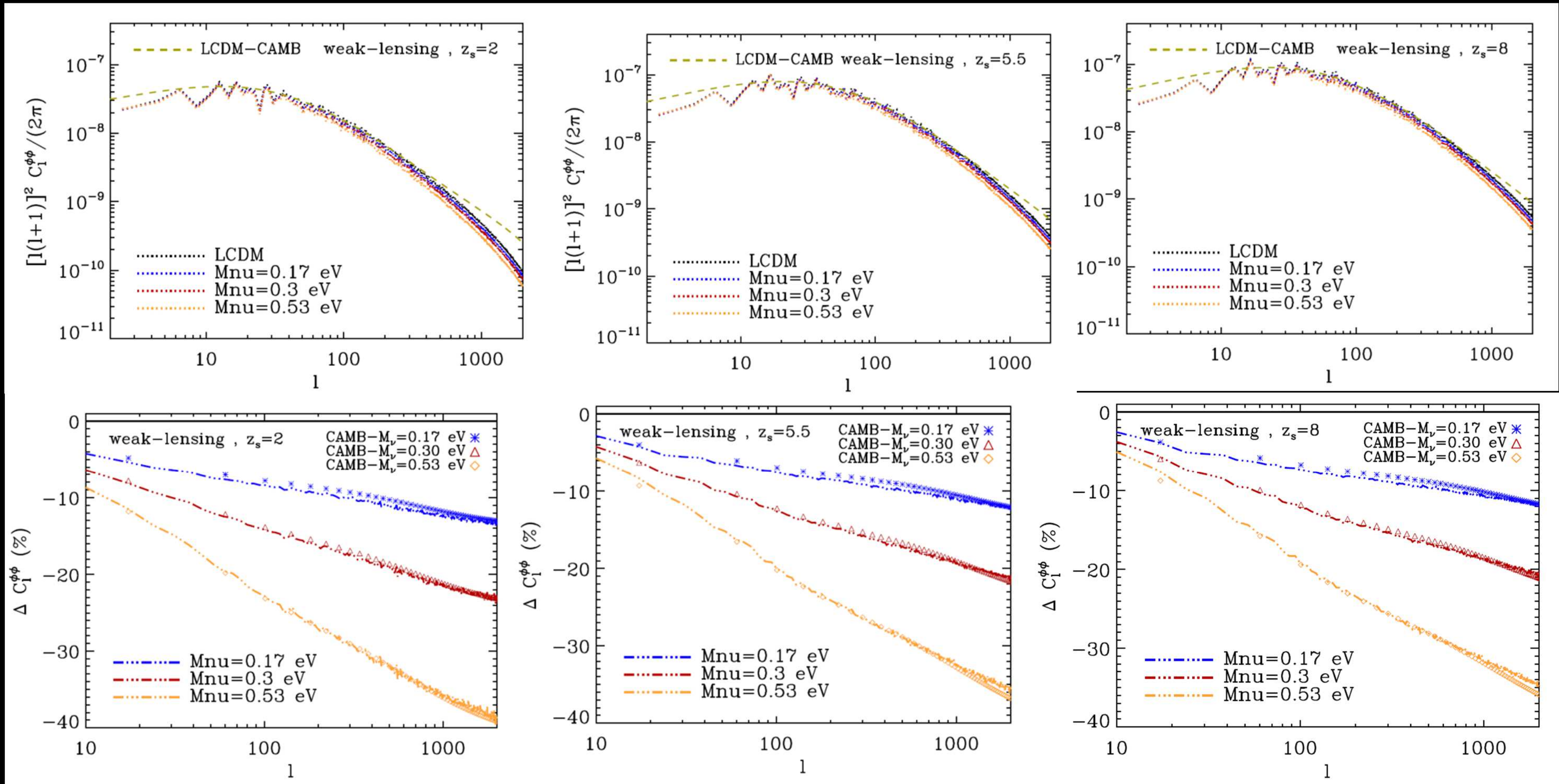

CC et al. in prep

Lack of power on small scales due to grid resolution.
The neutrino damping effect is correctely recovered up to *l*=2000

CMB-lensing angular power spectra

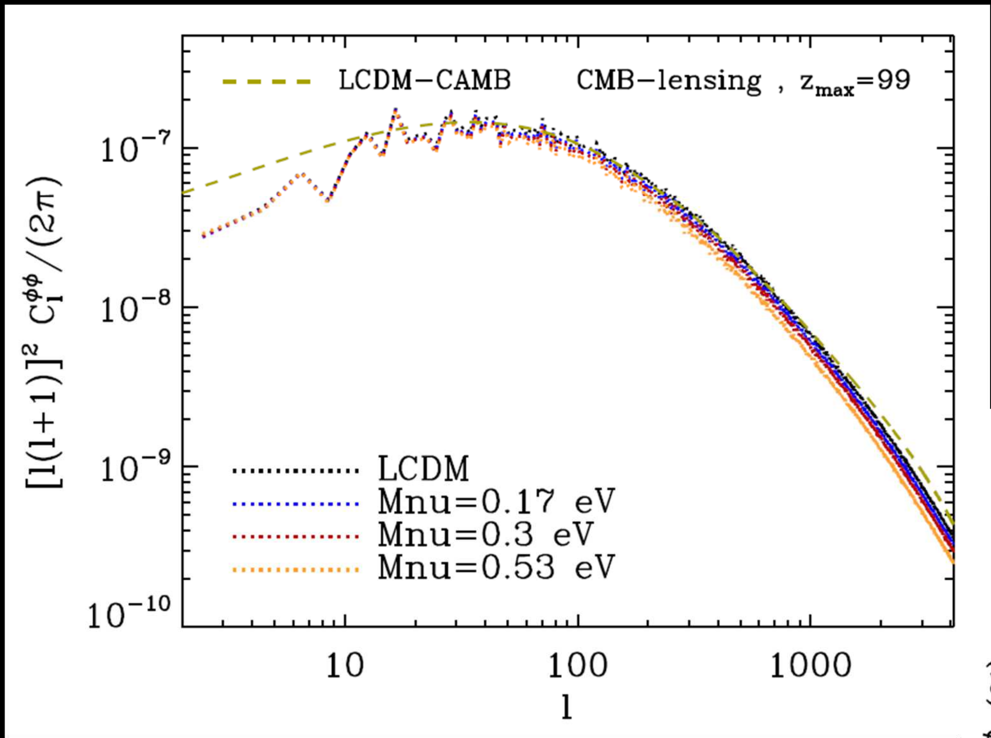

Power suppression is less than in the weak-lensing case since there is the contribution from higher z

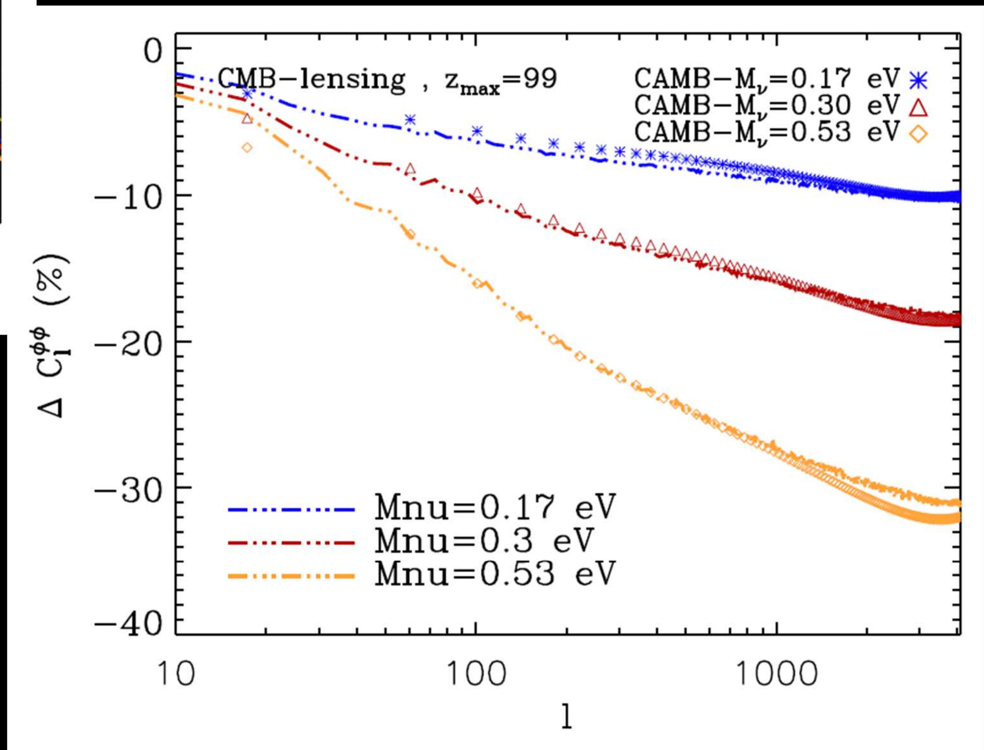

CC et al. in prep

CMB-lensing vs ISW-RS

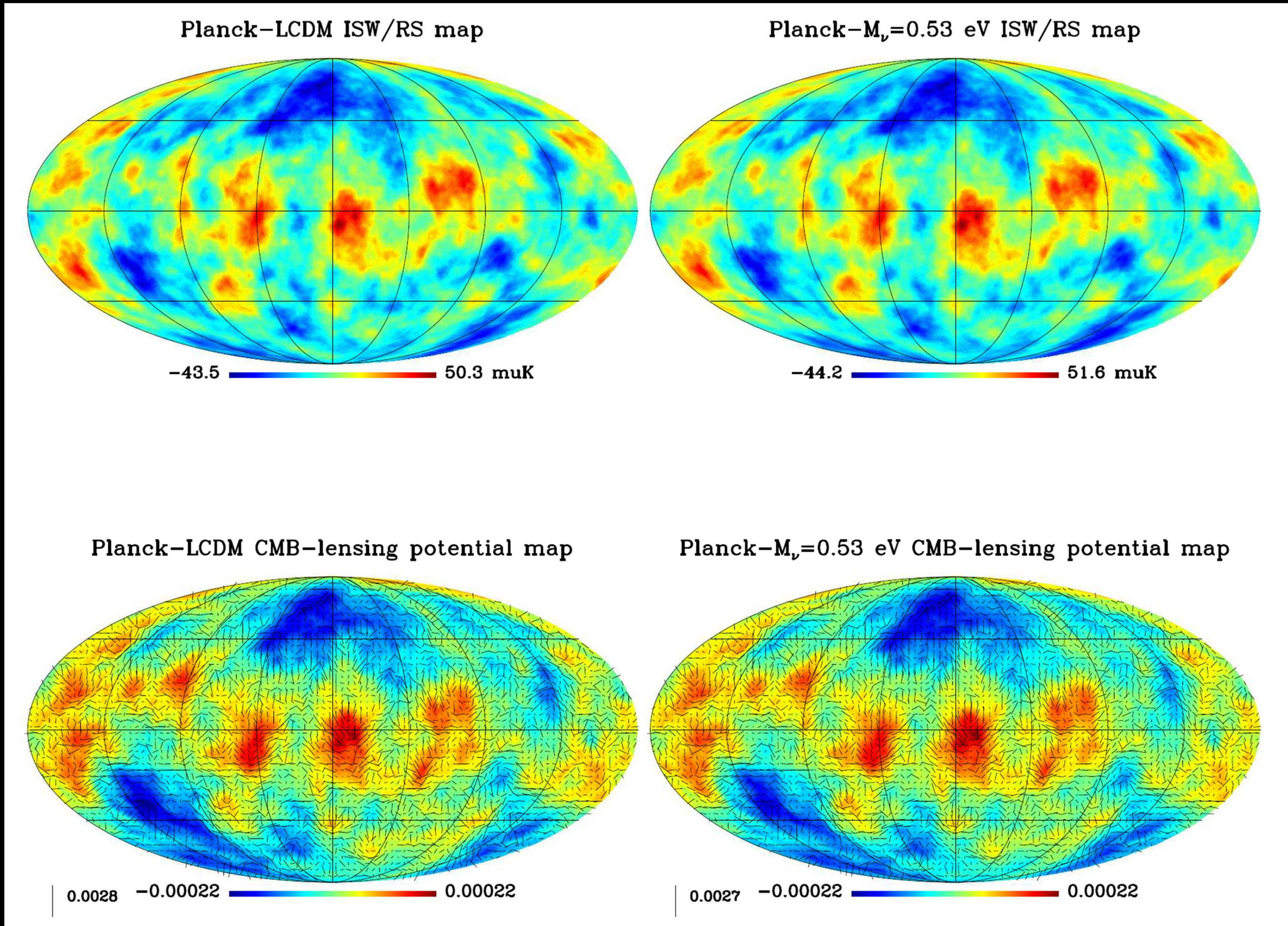

CC et al. in prep

ISWRS angular power spectra

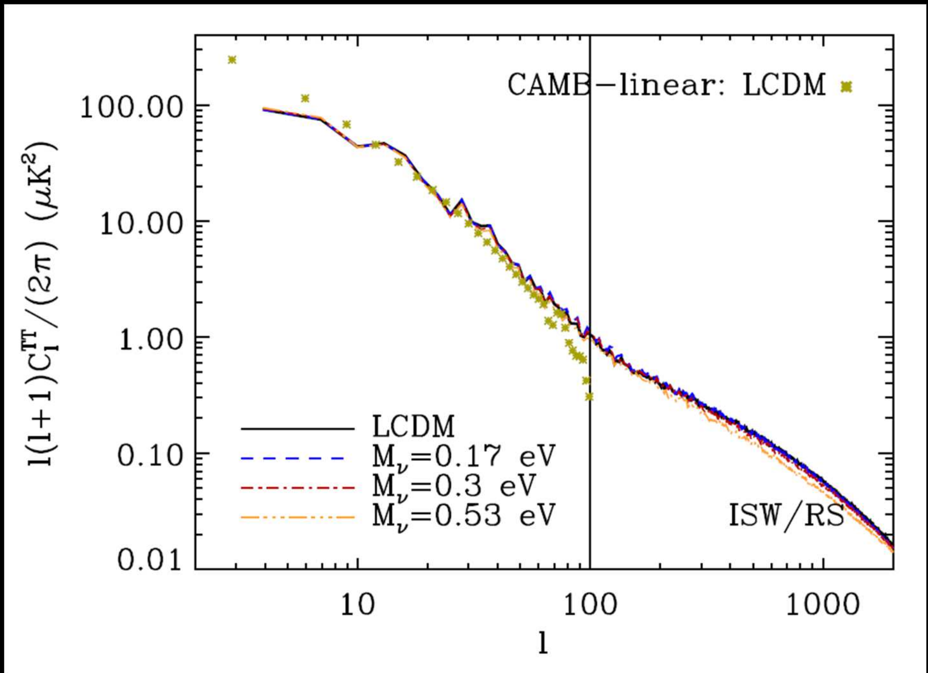

At high redshift, the ISW effect would be null on all scales for M_ν=0, while for M_ν>0 it is still active on small scales because of free-streaming.

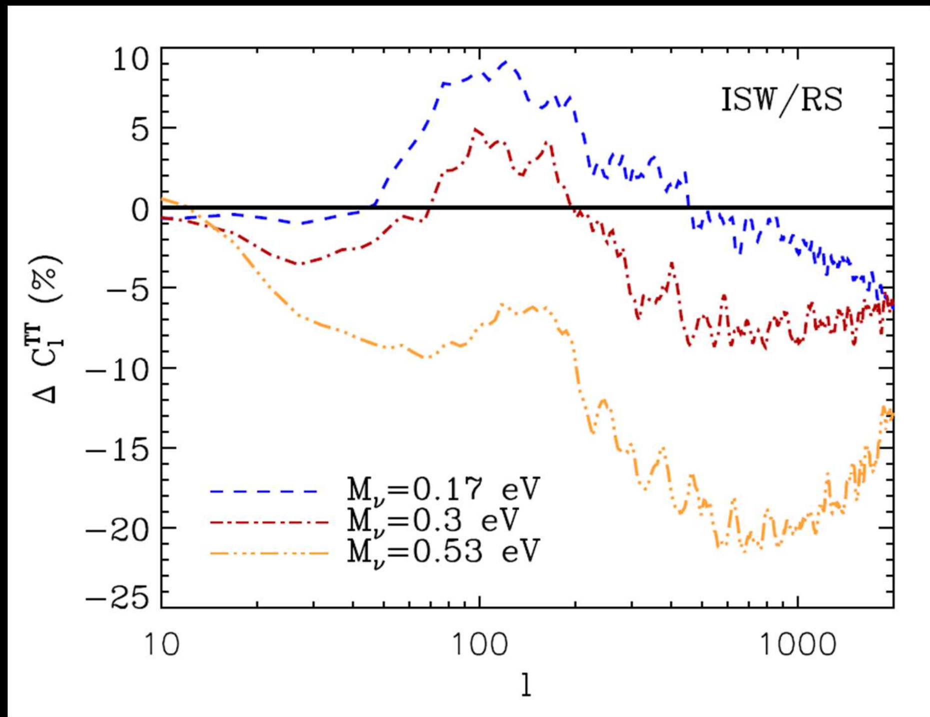

CC et al. in prep

ISWRS angular power spectra at different redshifts

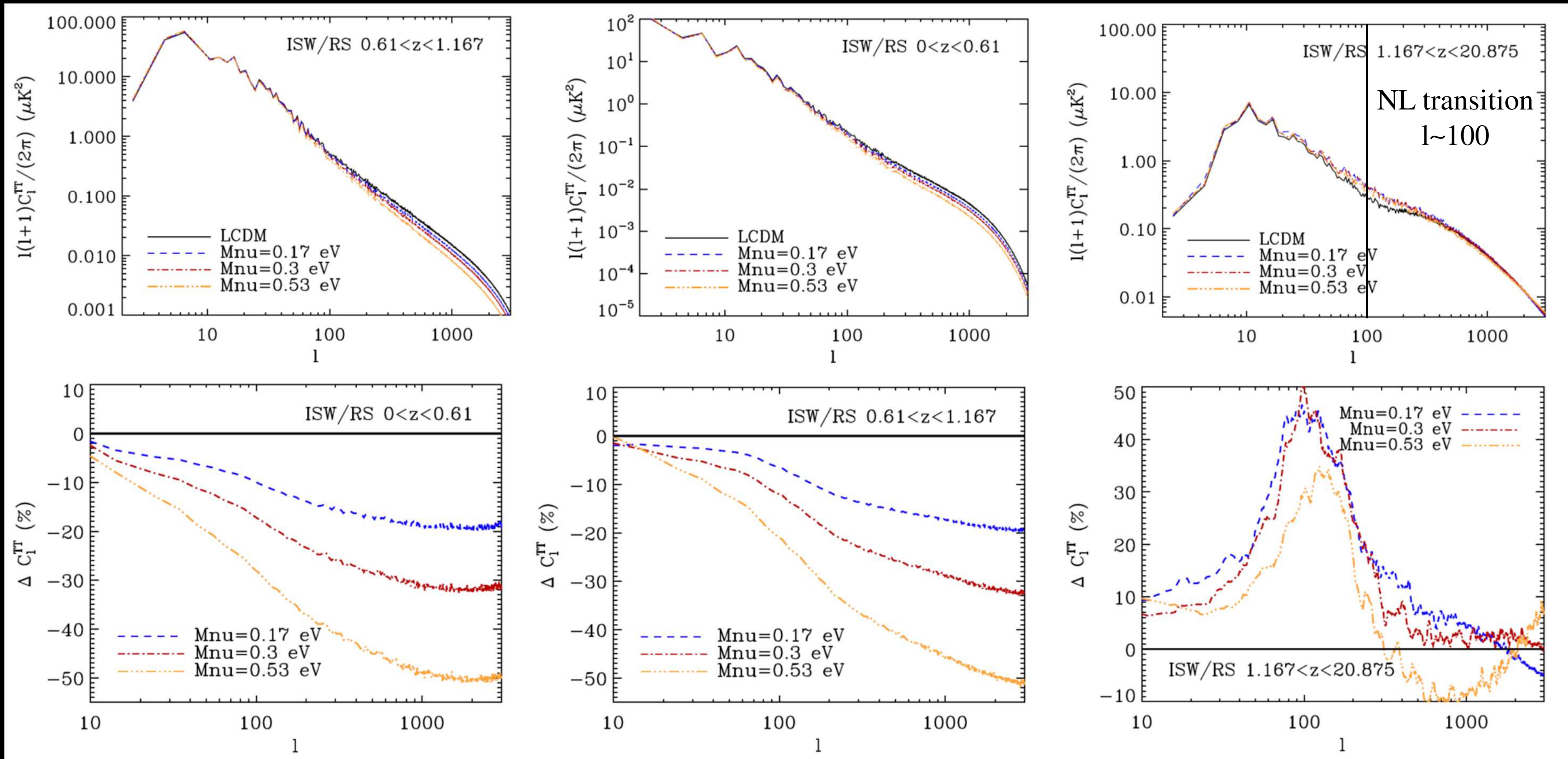

CC et al. in prep

At redshifts non DE-dominated there is an excess of power

$$k_{\rm fs}(z) = 0.82 H(z)/H_0/(1+z)^2 (m_\nu/1{\rm eV})\ h\,{\rm Mpc}^{-1}$$

ISWRS-CMBlens cross correlation

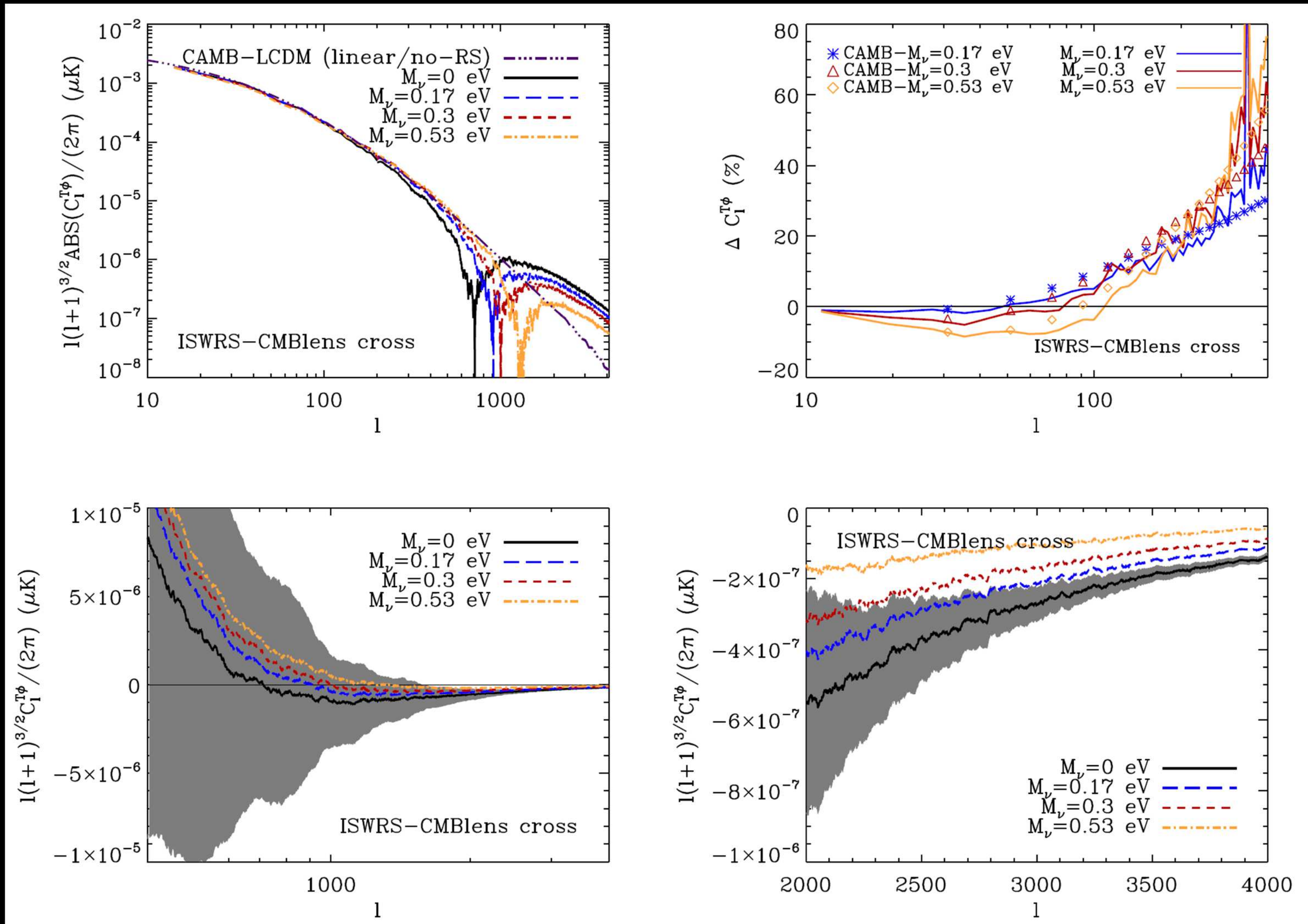

CC et al. in prep

Sign inversion: the non-linear transition moves toward smaller scales with increasing neutrino mass

ISWRS-Weaklens cross correlation

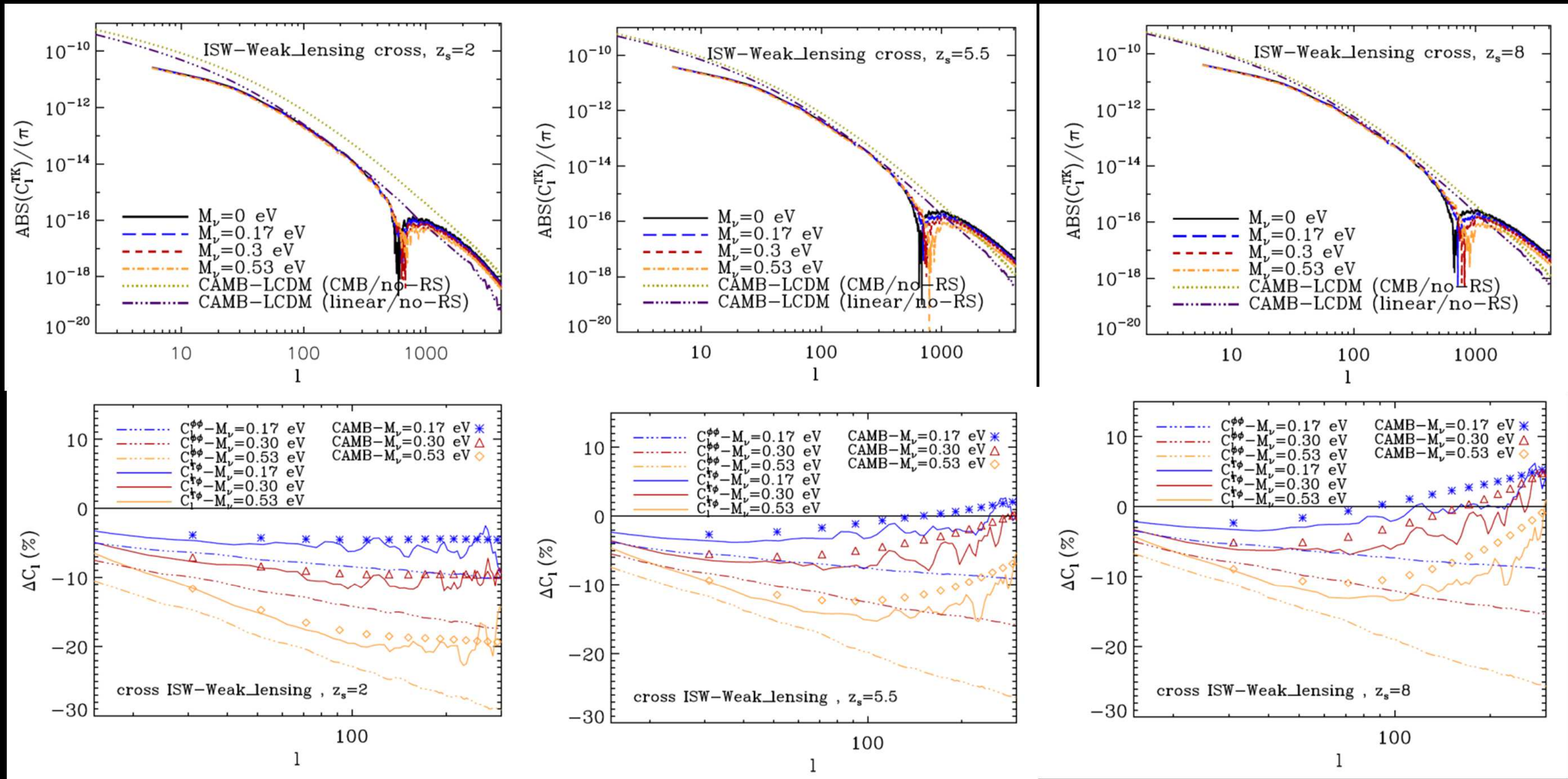

CC et al. in prep

Difference depends on the source redshift. Excess of power of the cross signal with respect to the auto-correlation signal.

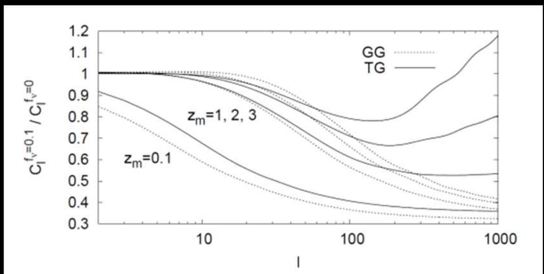

FIG. 2: Ratio of the cross-correlation multipoles C_l^{TG} and auto-correlation multipoles C_l^{GG} obtained for two cosmological models with neutrino density fractions equal to $f_\nu = 0.1$ or 0, and the same value of other cosmological parameters (see the text for details).

(Lesgourgues et al. 2008)

ISW-galaxy correlation predictions as function of the median redshift

Conclusions

- ✓ **Very large neutrino simulations for different probe combinations**
- ✓ **Previous results on bias and MF recovered and confirmed**
- ✓ **New Halofit prescription to account for massive neutrinos**
- ✓ **Good behaviour of exiting PT approximations if applied to CDM alone.**
- ✓ **Detection of the scale dependent growth-rate at linear scales**
- ✓ **Suppression of the CMB/weak-lensing signals, depending on the neutrino mass and source redshifts**
- ✓ **Enhancement of power at the ISW-RS transition of about 10% due to neutrino free-streaming**
- ✓ **Enhancement of the ϕT cross-correlation in the case of the CMB lensing-potential, and for high redshift lensed sources, depending on the neutrino mass**
- ✓ **Suppression of ϕT cross-correlation for low median redshift surveys, but anyway larger than $\phi\,\phi$ auto-correlation.**